Feedback Control Scheme for Scanning X-Ray Topography

Cite as: Journal of Applied Physics **43**, 687 (1972); https://doi.org/10.1063/1.1661177
Submitted: 24 February 1971 • Published Online: 10 November 2003

L. J. van Mellaert and G. H. Schwuttke

Feedback Control Scheme for Scanning X-Ray Topography*

L.J. van Mellaert† and G.H. Schwuttke
IBM Corporation, East Fishkill Laboratories, Hopewell Junction, New York 12533
(Received 24 February 1971; in final form 20 August 1971)

Feedback control of scanning x-ray topography is described. A control scheme is developed that maintains the x-ray topography system at all times at the peak of the rocking curve $I(\beta)$. The mathematical control scheme is implemented through an angular derivative generator capable of generating the signal $dI/d\beta$ on a continuous basis. Circuit requirements to measure $dI/d\beta$ continuously are established. Actual measurement of the command signal $dI/d\beta$ is accomplished through a modulation technique. Circuit design details are given and the operation of the system is discussed.

I. INTRODUCTION

Scanning x-ray topography is a well-known technique for the investigation of nearly perfect crystals.[1] A major problem in scanning x-ray topography is caused by the presence of long-range strain fields in crystals. Such strains make it difficult or impossible to obtain large-area topographs of entire crystal slices. To overcome such difficulties, the scanning oscillator technique (SOT) was introduced.[2] This technique has produced excellent topographs of silicon crystal slices as large as 150 mm in diameter, but SOT recording times are at least twice as long as required for the standard scanning transmission techniques. Recently, an improvement of the scanning oscilator technique was described.[3]

The new approach based on feedback control of the topographic camera results in minimum exposure time, less background scatter, and better contrast in the topographs.

The purpose of this paper is to present more details on feedback control as applied to x-ray topography. An adaptive control scheme is described that keeps the "operating point" of the Bragg reflection at all times at the maximum of the "rocking curve"[4] $I(\beta)$. This is accomplished by generating the angular derivative signal $dI/d\beta$ on a continuous basis. Circuit requirements to measure $dI/d\beta$ continuously are extablished. Actual measurement of the command signal $dI/d\beta$ is accomplished through use of a simple sinusoidal perturbation signal $\sin\alpha t$.

II. CONTROL SCHEME FOR X-RAY TOPOGRAPHY

X-ray topography deals with nearly perfect crystals. The crystals are of finite thickness and are investigated with monochromatic x-rays. Diffraction patterns of such crystals are very complex and are given by the dynamical theory of x-ray diffraction.[5] Experimentally, diffraction patterns are measured as reflection or rocking curves $I(\beta)$ by rotating the crystal through the exact Bragg angle. A rocking curve of silicon, 220 reflection, recorded with molybdenum radiation typical for our experimental conditions is shown in Fig. 1.

For the following it is useful to summarize some important properties of rocking curves.[4] Evidently, the reflected intensity I is a symmetric function of the angular deviation β. The diffracted intensity is maximum for $\beta=0$. The shape of the rocking curve is independent of the direction of the diffraction vector. Normally a small change of lattice parameter does not change the width and shape of a rocking curve. However, such a lattice parameter change may shift the Bragg angle of the operating reflection by an amount large compared with the theoretical half-widths of the rocking curve.

Automatic control of the x-ray system ensures operation of the diffraction system at the peak of the rocking curve ($\beta=0$). Conventional automatic control systems use sensor devices, such as transducers, to measure directly the deviation of the controlled system from the desired operating point because the output signal of the sensor is usually a monotonic function of the error. In contrast to conventional control functions, the rocking curve is a symmetric function. Therefore, two values of β correspond to every single value of I. Consequently, it is not possible to decide from one measurement of the intensity I in which direction β should be adjusted to make the diffraction system operate at the peak of the rocking curve. A monotonic function that could exert the desired control function is the angular derivative of the rocking curve $dI/d\beta$. If $dI/d\beta$ can be measured continuously, a control system can be designed to adjust β such that $dI/d\beta=0$. A simplified system of this kind is shown in the diagram of Fig. 2. There the angular derivative signal $dI/d\beta$ is integrated and the output of this integrator is used as a drive signal of the angular actuator on which the crystal to be

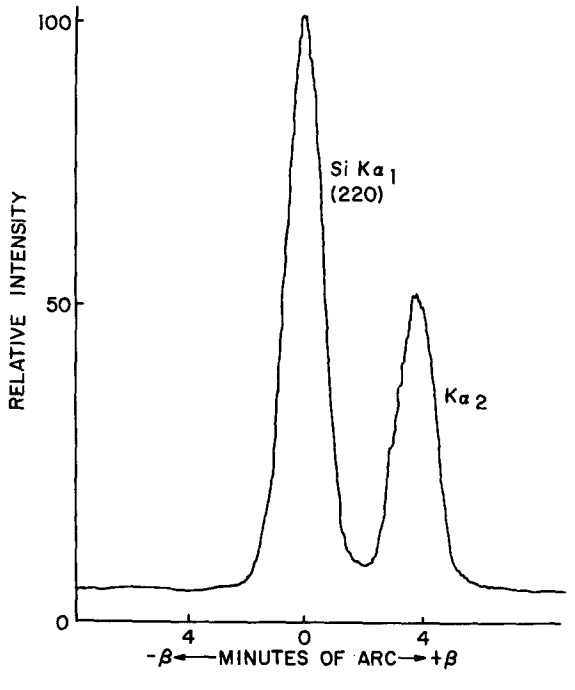

FIG. 1. Typical rocking curve $I(\beta)$, 220 reflection in silicon, Mo radiation.

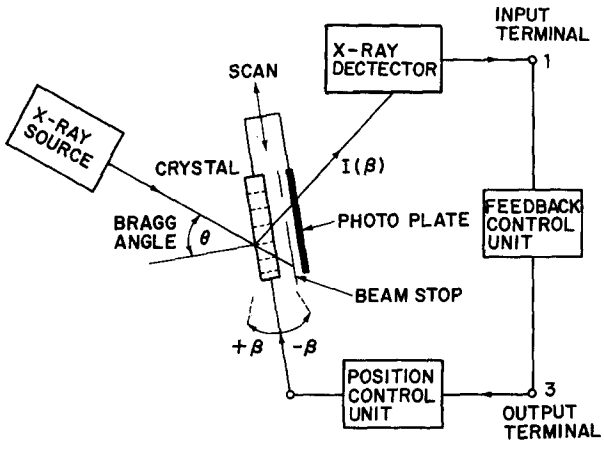

FIG. 2. Schematic of automatic Bragg-angle control (ABAC) system.

analyzed is mounted.[3] The relationship between $dI/d\beta$ and β imposed by the control system is given by

$$\beta(t) = K\int_{t_0}^{t} \frac{dI}{d\beta}(t')\,dt', \tag{1}$$

in which K represents the integrator gain constant and t the time variable. Taking the derivative of this expression with respect to time it follows that

$$\frac{d\beta}{dt} = K\frac{dI}{d\beta}, \tag{2}$$

and for $\beta = 0$,

$$\frac{d\beta}{dt} = K\frac{dI}{d\beta}\bigg|_{\beta=0} = 0. \tag{3}$$

From Eq. (2) it is seen that β is adjusted in the direction of I. For $\beta = 0$, Eq. (3) shows that $d\beta/dt = 0$, therefore, the system will operate at the peak of the rocking curve. Thus, the control scheme is straightforward, provided a suitable method can be found for generating the angular derivative signal $dI/d\beta$ on a continuous basis. In automatic control theory, the system described here would fall into the class of optimizing systems generally known as hillclimbing systems. Such control systems are described under various forms in the literature.[6]

In designing the circuit of a continuous-derivative generator it is useful to recall that the derivative of a function is not a property of a single point of this function, but expresses the behavior of a function in the vicinity of the point at which the derivative is defined. In practice, a derivative is approximated by a perturbation of the operating point. However, in contrast to the rigor of mathematical reasoning, it is not possible to make arbitrary small excursions around the operating point because instrumentation and noise introduce errors that make it impractical to operate the circuit below a certain limit. Taking this into consideration it follows that the feedback control unit must be capable of continuous exploration of the response $I(\beta)$ in the direct vicinity of the momentary value of β. This value of β is called the operating point β^*.

The practical measurement of $dI/d\beta$ requires a perturbation $p(t)$ around the operating point β^*. In the reported system, the perturbation is a sinusoidal signal $p(t) = A\sin\alpha t$. This signal was chosen because of the convenience of implementation.

The response of the x-ray intensity $I(\beta)$ to the perturbation can be expressed for a sufficiently small perturbation amplitude A in the form of a Taylor series expression about β^*:

$$I(\beta) = I(\beta^*) + \frac{\partial I}{\partial\beta}\bigg|_{\beta^*} A\sin\alpha t + \frac{1}{2}\frac{\partial^2 I}{\partial\beta^2}\bigg|_{\beta^*} A^2\sin^2\alpha t + \cdots \tag{4}$$

Recovery of $(dI/d\beta)|_{\beta^*}$ is easily accomplished by multiplying the signal $I(\beta)$ with the perturbation signal $\sin\alpha t$ and passing the product signal through an appropriate low-pass filter. This principle is illustrated in Fig. 3 which is a detailed diagram of the block labeled "feedback control unit" as shown in Fig. 2.

Upon multiplying both sides of (4) with $\sin\alpha t$ we get

$$I(\beta)\sin\alpha t = I(\beta^*)\sin\alpha t + \frac{\partial I}{\partial\beta}\bigg|_{\beta^*}\frac{A}{2}(1-\cos 2\alpha t) + \frac{1}{2}\frac{\partial^2 I}{\partial\beta^2}\bigg|_{\beta^*} A^2\sin^3\alpha t + \cdots \tag{5}$$

If the signal $I(\beta)\sin\alpha t$ is passed through a low-pass filter with a cutoff frequency below α, the only component of significance in the filter output is the dc component present in the second term

$$\frac{A}{2}\frac{dI}{d\beta}\bigg|_{\beta^*}$$

because, additional dc output components will rapidly vanish with decreasing values of the amplitude A due to the even-power terms of $\sin\alpha t$ in (5). In practice, the multiplication is done by means of a square-wave signal because instrumentation of a square-wave signal is much simpler than of a sinusoidal signal. From a Fourier-series expansion of the square-wave signal, it follows readily that the above analysis is also valid for the square wave.

III. CIRCUIT DETAILS OF FEEDBACK CONTROL UNIT

The schematics of a feedback control unit which implements the mathematical operation described in Sec. II is shown in Fig. 3. Its input terminal (1) and output terminal (3) are connected between like-numbered terminals in Fig. 2. The input terminal receives the signal I from the x-ray detector (Fig. 2). Since the signal

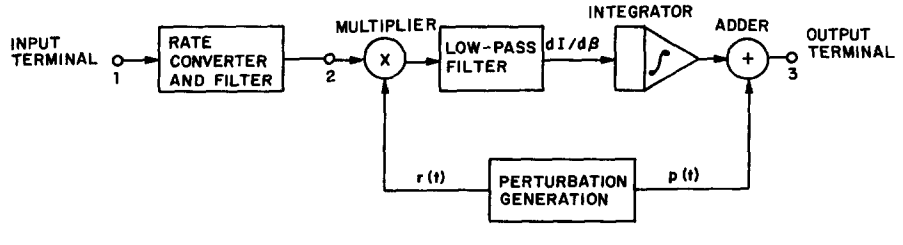

FIG. 3. Diagram of feedback control unit shown in Fig. 2.

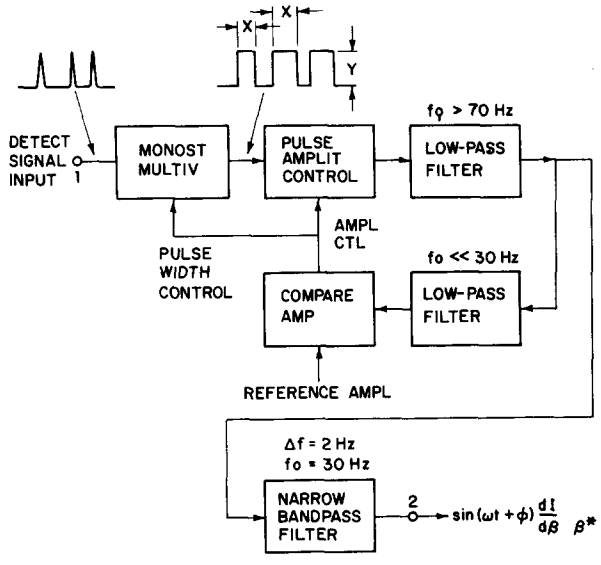

FIG. 4. Diagram of rate converter and filter.

I from the detector is inconveniently in the form of spike pulses and is also in an environment of noise, the rate converter and filter circuit is employed to precondition the signal before the correlation in the multiplier. The output of the rate converter circuit at the terminal (3) is in the form of $(\sin\alpha t)(dI/d\beta)$ at β^*. The rate converter and the filter circuit is shown in more detail in Fig. 4. The rate converter incorporates an automatic gain control circuit which maintains the amplitude of the detected perturbation signal at a constant level. This is necessary because otherwise the effective gain constant K in Eq. (1) would be dependent upon the x-ray intensity captured by the detector. Due to the intensity variations encountered in the scanned crystals, the dynamical behavior of the control system would vary with these intensity fluctuations.

The multiplier X in Fig. 3 functions to carry out the correlation of the detected signal at the terminal 2 with a signal $r(t)$ derived from the perturbation signal $p(t)$ both generated in the perturbation generator. A conventional low-pass filter operates to select the value $dI/d\beta$ at β^* from the output of the multiplier. With the perturbation signal $p(t)=\sin\omega t$ and $\omega=\alpha$, the cutoff frequency of the low-pass filter is below α. For our system $\alpha=30$ Hz.

The output of the low-pass filter is fed to a conventional integrator ($\int$ in Fig. 3). The output of the integrator $\int$ is a current $i(\beta^*)$ which is fed as one component of the current "i" to the coils of the position control unit[3] shown schematically in Fig. 5. The component $i(\beta^*)$ operates to hold the crystal at a position such that β equals β^*. If β^* is less than zero, the signal $dI/d\beta$ at β^* from the low-pass filter is positive and, therefore, the integrator increases the value of $i(\beta^*)$. If $dI/d\beta$ is negative from the low-pass filter, the integrator functions to decrease the value of $i(\beta^*)$ so that again β^* approaches zero. If β^* equals zero, $dI/d\beta$ from the low-pass filter is also zero and the output of the integrator remains constant.

Added to the component current $i(\beta^*)$ from the integrator is the perturbation signal $p(t)$ from the perturbation generator. The adder is conventional and the current i fed to the position control unit of Fig. 2 is $i[\beta^*+p(t)]$. The perturbation generator in our system includes a conventional sine-wave generator for generating the signal $p(t)=\sin\alpha t$.

For simplicity, the amplitude of the $\sin\alpha t$ perturbation signal is ignored but, of course, the amplitude is selected such that the variation of β about β^* as caused by $p(t)$ is not excessive. As a general rule with reference to Fig. 6, variations of β about β^* should not exceed β_1 or β_2. The presence of the $K\alpha_2$ peak (Fig. 1) does not cause any difficulties in the control because the perturbation around $K\alpha_1$ is much less than the (4 min) separation between $K\alpha_1$ and $K\alpha_2$. Appropriate means for adjusting the amplitude of $i[p(t)]$ with respect to $i(\beta^*)$, such that excessive variations of β do not occur, are included within the perturbation generator. Usually variations of β caused by $p(t)$ will be much less than β_1 and β_2.

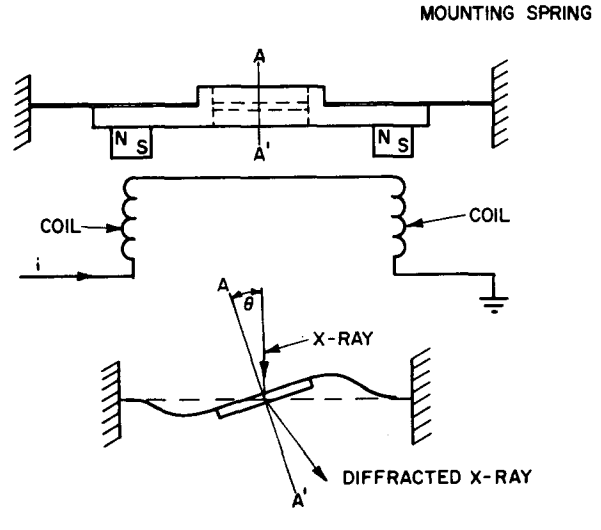

FIG. 5. Schematic of position control unit. For details see Ref. 3.

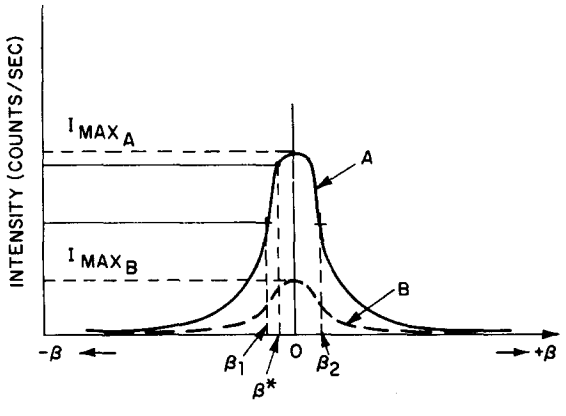

FIG. 6. Rocking curves $I(\beta)$ for different peak values showing operating point β^*.

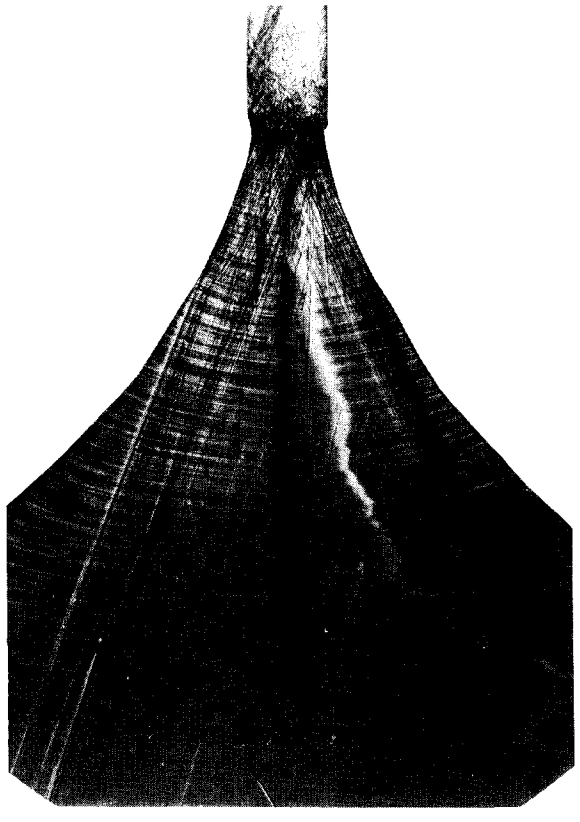

(a)

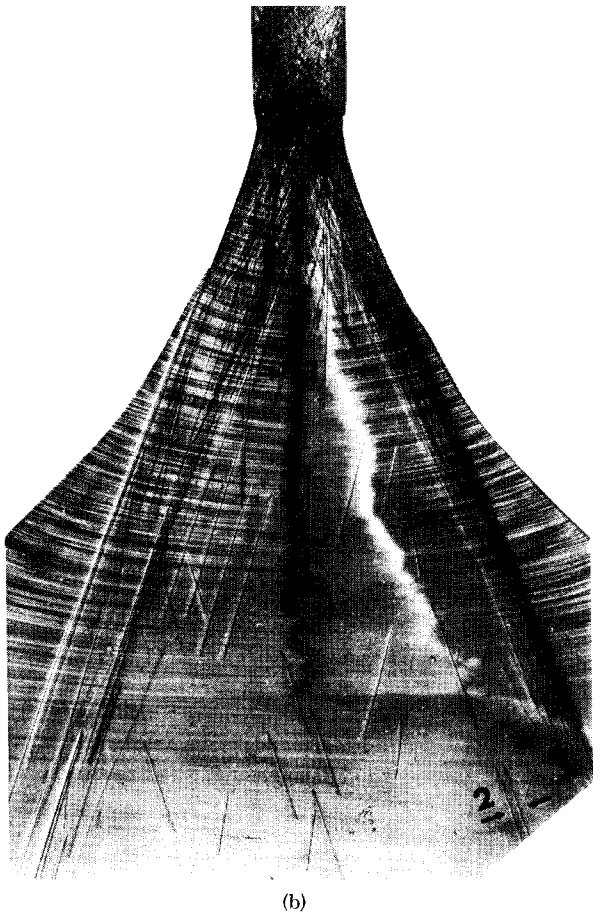

(b)

FIG. 7. X-ray topograph of silicon slice showing impurity segregation and dislocations: (a) recorded without system; (b) ABAC recorded.

IV. SYSTEM OPERATION

Since some of the details of operation have already been discussed in connection with the circuit description, this section describes the operation in a summary fashion. Reference is made to Figs. 2 and 3. At the start of the operation a crystal is placed in the position control unit. Thereafter, the crystal and the position control unit are rotated such that the x-ray beam is incident at the exact Bragg angle θ and the diffracted beam is detected by the x-ray detector.

Subsequently, the perturbation generator is started to generate the signal $p(t)=\sin\alpha t$, where $\alpha=30$Hz. The perturbation signal is added in the adder with some initialization value $i(\beta^*)$ obtained from the integrator to form the current i which is supplied to the coils (shown schematically in Fig. 5) of the position control unit. This current i equals $i[\beta^*+p(t)]$, where the component $i(\beta^*)$ holds the crystal at the operating point β^* and the component $i[p(t)]$ causes the crystal to oscillate about β^* with the frequency of $\sin\alpha t$. The magnitude of the oscillation about β^* is such that the average intensity variation in the diffracted beam is insignificant. For example, a variation in intensity not greater than 10% of the difference in intensity between $I(\beta)_{\beta=0}$ and $I(\beta_1)$, as discussed in connection with curve A of Fig. 6, would not be significant. With the control unit in operation, the scan motor is initiated to scan the crystal back and forth between the extreme translation positions L1 and L2.

The x-ray detector forms a signal I at its output which is converted and filtered in the rate converter of Fig. 3 to form at terminal 2 the signal $\sin(\alpha t+\phi)\,(dI/d\beta)$ at β^*. The multiplier multiplies the signal at terminal 2 with the square-wave signal $r(t)$ as derived from the perturbation generator (Fig. 3). The multiplication provides a signal which is passed through the low-pass filter having a cutoff frequency of 2α to form the derivative $\frac{1}{2}A\,(dI/d\beta)|_{\beta^*}$. The signal from the low-pass filter is integrated in the integrator $\int$ to form the component signal $i(\beta^*)$ which is again added with the signal $p(t)$ in the adder to form the current i. The output from the

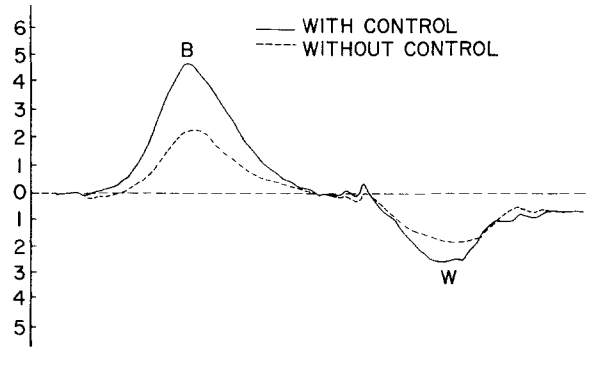

FIG. 8. Densitometer trace of sample shown in Figs. 7(a) and 7(b) taken at position 1 across impurity segregation. Dashed line corresponds to Fig. 7(a). Solid line corresponds to Fig. 7(b).

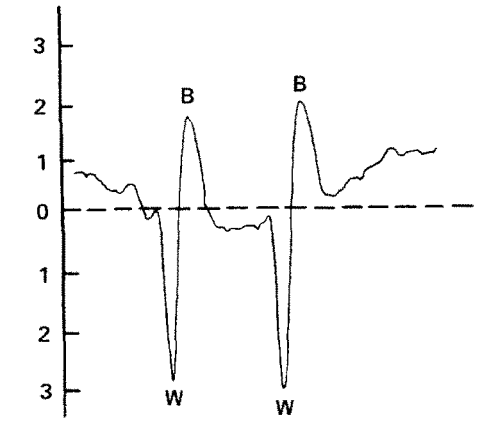

(a)

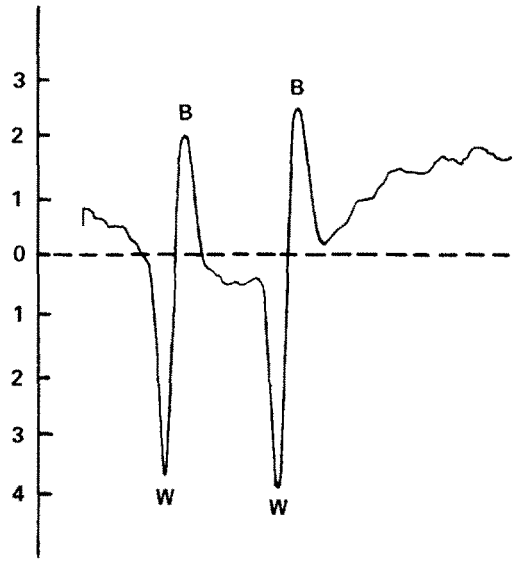

(b)

FIG. 9. Densitometer trace of sample shown in Fig. 7 at position 2 across two dislocation lines: (a) corresponds to Fig. 7(a); (b) corresponds to Fig. 7(b).

integrator $\int$ continually changes such that the component current $i(\beta^*)$ continually adjusts β such that β^* tends to equal zero.

V. APPLICATIONS

An automatic Bragg-angle control (ABAC) system has been in operation in our laboratory for a period of several years. During that period the system was tested under many different conditions and excellent results were obtained. Pertinent examples related to the recording of x-ray topographs of silicon wafers, such as the recording of topographs of entire wafers in the presence of elastic strains, the reduction of scattering background in topographs, and savings in recording time of topographs are discussed in Ref. 3. Two additional examples illustrating "dynamical image contrast" are given here. The first one is related to silicon and the second one to germanium. Both examples demonstrate improvements in topograph quality obtained through ABAC. Improvements in strain contrast due to impurity segregation and dynamical dislocation contrast are shown in Fig. 7. The topographs shown in Figs. 7(a) and 7(b) were obtained from a silicon slice cut as follows: After growing a ⟨111⟩ silicon crystal, a 1-mm-thick slice was cut out of its center parallel to the ⟨111⟩ growth axis. The cut was made in a (112) plane through the center of the ingot and also through the seed. Accordingly, a topograph of such a slice shows the impurity segregation in the growing crystal and also dislocations in the seed and their propagation into the growing crystal. The topograph in Fig. 7(a) was recorded without the system in operation. Figure 7(b) represents the topograph recorded with the system working. The over-all improvement in constrast in the ABAC topograph compared to the standard topograph

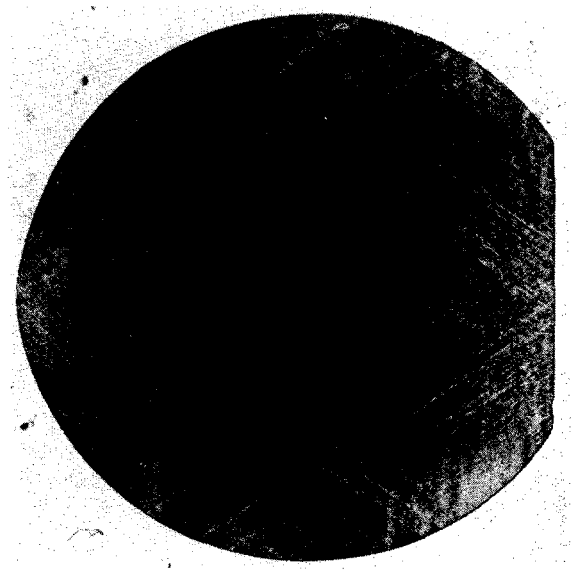

(a)

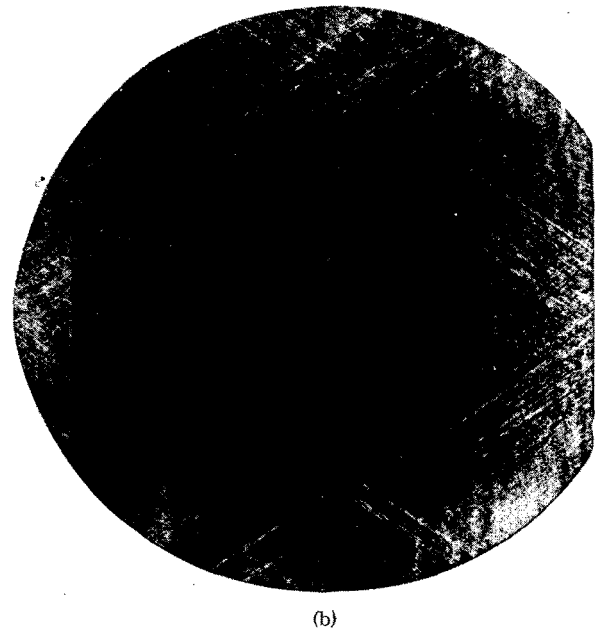

(b)

FIG. 10. X-ray topographs of germanium slice covered with silicon oxide film: (a) recorded without system; (b) ABAC recorded.

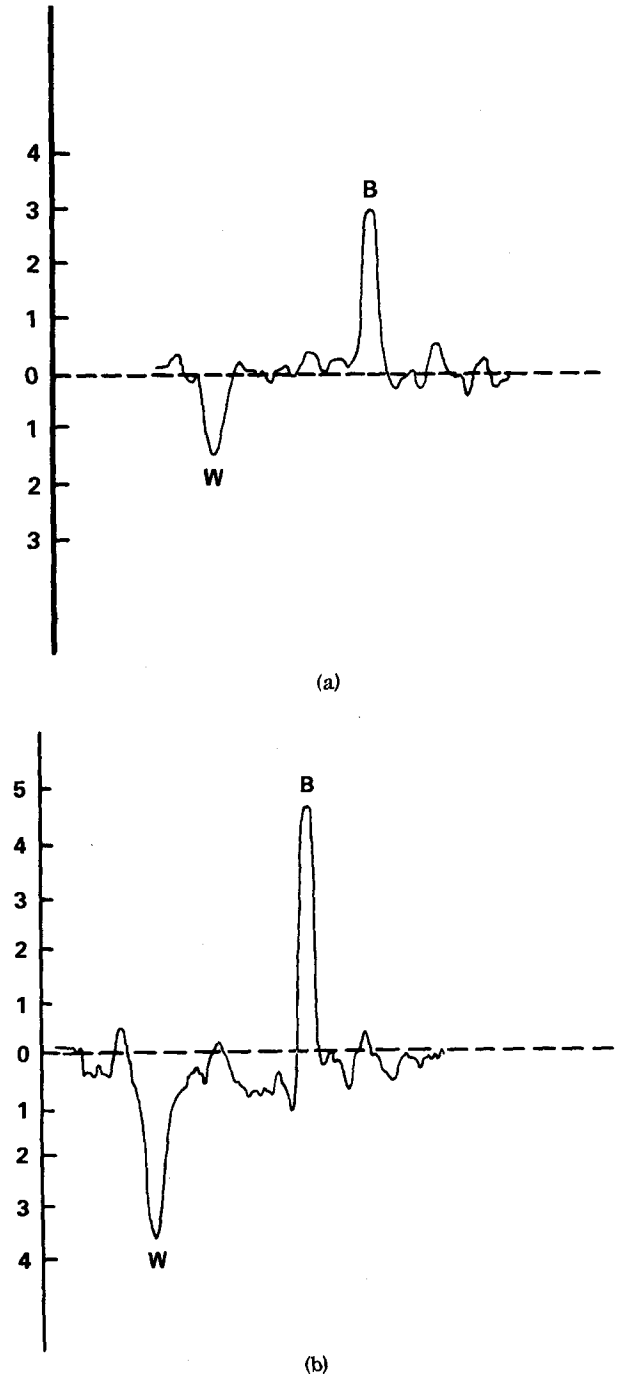

FIG. 11. Densitometer traces across window edges taken at position indicated in Fig. 10: (a) recorded without system; (b) ABAC recorded.

can be recognized in the pictures. The contrast improvement follows more readily from the densitometer traces taken at the position indicated in Figs. 7(a) and 7(b). Figure 8 shows the trace taken at position 1 and Figs. 9(a) and 9(b) the trace taken at position 2.

An example related to germanium is given in Figs. 10(a) and 10(b). The superior dynamical image contrast in ABAC recorded Ge topographs is also evident here. Dynamical image contrast is displayed along window edges cut into SiO_2 films deposited on germanium.[7] The SiO_2 film used for this experiment was grown approximately 2250 Å thick on a (111) germanium slice. The germanium wafer is 0.3 mm thick resulting in $\mu_0 t \sim 10$ for Mo$K\alpha$ radiation (μ_0 is the linear absorption coefficient for Mo$K\alpha$; t is the sample thickness). After oxide deposition triangular-shaped windows were opened in the film through standard photolithographic techniques. The triangle sides in the topographs of Fig. 10 are 5 mm long and parallel to the ⟨110⟩ and ⟨112⟩ directions in the (111) wafer plane. The photodensitometer traces taken at the position indicated in the topograph (arrow) are given in Fig. 11 and show clearly the improved image quality. Similar improvements have also been achieved with GaAs crystals.

ACKNOWLEDGMENT

We are indebted to H.F. Ilker for technical assistance in building the control system.

---

*Work supported in part under Air Force Contract, Air Force Cambridge Research Laboratories, Bedford, Mass.
†Present address: RCA: s.a. Parc Industrial des Hauts Sarts 4400 Herstal-Liege-Belgium.
[1]A.R. Lang, J. Appl. Phys. 29, 597 (1958).
[2]G.H. Schwuttke, J. Appl. Phys. 36, 2712 (1965).
[3]L.J. van Mellaert and G.H. Schwuttke, Phys. Status Solidi 3, 687 (1970).
[4]A.H. Compton and S.K. Allison, *X-Rays in Theory and Experiment* (Van Nostrand, New York, 1935).
[5]M.V. Laue, Röntgenstrahlinterferenzen (Akademische Verlagsgessellschaft, Frankfurt/Main, 1960); R.W. James, in *Solid State Physics*, edited by F. Seitz and D. Turnbull (Academic, New York, 1963), Vol. 15.
[6]E. Mishkin and L. Braun, *Adaptive Control Systems* (McGraw-Hill, New York, 1961).
[7]G.H. Schwuttke and J.K. Howard, J. Appl. Phys. 39, 1581 (1968).